

Repeated Century-Scale Droughts over the Past 13,000 Years near the Hudson River Watershed, U.S.A.

Paige E. Newby^{a,1}, Bryan N. Shuman^b, Jeffrey P. Donnelly^c, Dana MacDonald^a

^aDepartment of Geological Sciences, Brown University, Providence, Rhode Island 02912;

^bDepartment of Geology and Geophysics, University of Wyoming, Laramie, Wyoming 82071;

^cDepartment of Geology and Geophysics, Woods Hole Oceanographic Institution, Woods Hole, Massachusetts 02543

¹To Whom Correspondence should be addressed:

Department of Geological Sciences, Brown University, 324 Brook Street, Box 1846, Providence, RI 02912

(w) 401-863-3659, (f) 401-863-3058

E-mail: Paige_Newby@brown.edu

Key words: lake level, Northeastern USA, hydroclimate, Holocene

Abstract

Sediment and ground-penetrating radar data from Davis Pond near the Hudson River valley reveal past droughts in a historically humid region that presently supplies water to millions of people in and around New York City. A minimum of eleven sandy paleoshoreline deposits in the lake date from 13.4-0.6 cal ka BP. The deposits span 1500 to 200 years between bracketing radiocarbon dates, and intrude into lacustrine silts up to 9.0 m below the modern lake surface in a transect of six cores. Three lowstands, ca. 13.4-10.9, 9.2 and 8.2 cal ka BP indicate low regional moisture balance when low temperatures affected the North Atlantic region. Consistent with insolation trends, water levels rose from ca. 8.0 cal ka BP to present, but five low stands interrupted the rise and are likely associated with ocean-atmosphere interactions. Similar to evidence from other studies, the data from Davis Pond indicate repeated multi-century periods of prolonged or frequent droughts super-imposed on long-term regional trends toward high water levels. The patterns indicate that water supplies in this heavily populated region have continuously varied at multiple time scales, and confirm that humid regions such as the northeastern USA are more prone to severe drought than historically expected.

Introduction

Water is a vital resource for sustaining life, and an abundant water supply within many temperate humid regions, such as the northeastern United States (“New England”), is typically provided by precipitation throughout the year, principally from frontal systems and tropical storms. Future trends in precipitation for New England, relative to the observed record from AD1961-1990, also project an increase in annual precipitation (Hayhoe et al., 2007). Despite such historic and predicted abundance, however, societal usage can exceed the normal water supply (DeGaetano, 1999; Hill and Polsky, 2007), posing a continuing challenge for maintaining regional water availability. Furthermore, currently rising temperatures and changes in hydroclimate, such as less winter moisture in the form of snow and decreased snowpack, raise the possibility of an increase in drought frequency (Hayhoe et al., 2007).

Like other humid regions, the instrumental record for New England (Griffith, 1994; Hayhoe et al., 2007; Kinnison, 1931; Leathers et al., 2000; Namias, 1966) shows droughts of varying magnitude and longevity, which variously strained regional water resources and availability. Most prominent is the severest drought on record in AD 1962-1965, when, for example, New York City reservoirs were depleted to dangerously low levels (Andrews in Cook, 1982). Four of six subsequent droughts (post-AD 1965) also curtailed water supply, and initiated involuntary water restrictions in the New York City metropolitan area (http://www.nyc.gov/html/dep/html/drinking_water/index.shtml). Thus, despite the modern imprint of moist conditions, understanding the frequency and magnitude of paleo-droughts appears critical in light of potential changing water supply and rising populations.

Studies of late-Quaternary lake levels reveal that water supplies in regions like New England may indeed be prone to even larger magnitude variation than experienced historically. Records from the region show multi-millennial trends in water levels with lower-than-modern levels from 11.0-8.0 cal ka BP, intermediate levels from 8.0-5.5 cal ka BP, low levels from 5.5-3.0 cal ka BP and high levels from 3.0 cal ka BP to present (Almquist et al., 2001; Dieffenbacher-Krall and Nurse, 2005; Newby et al., 2000; Shuman et al., 2001, 2005; Webb et al., 1993). More recent work has emphasized the potential for sub-millennial scale hydroclimate variation within this regional framework. The closest study to the Hudson River watershed indicates four (ca. 1.3, 3.0, 4.4, 6.1 cal ka BP) centennial-scale droughts in New Jersey (Li et al., 2007), and two lakes in Massachusetts contain evidence of repeated century to multi-century droughts throughout the past 14.0 cal ka BP (Newby et al., 2009).

Here, we examine paleo-drought frequency by developing a centennial-resolution, lake-level history from Davis Pond (42°8.13'N, 73°24.46'W, 213 m elevation), a small (4 ha, 2 m maximum depth) surficially-closed basin 40 km east of the Hudson River and 60 km east of New York City's 122.9 billion gallon (0.465 km³) Ashokan Reservoir in the Catskill Mountains (http://www.nyc.gov/html/dep/html/watershed_protection/ashokan.shtml). Davis Pond is also located 175 and 230 km respectively from the detailed study locations at White Lake, New Jersey (Li et al., 2007) and on the Plymouth-Carver Sand Plain of Massachusetts (Newby et al., 2009; Shuman et al., 2009). Despite numerous local paleoenvironmental studies in the region (Kirby et al., 2002; Maenza-Gmelch, 1997; Peteet et al., 1990), no other paleohydrologic studies have been conducted at century-scale resolution within 350 km. Dendroclimatic data, however, indicate a series of multi-year droughts dating back 1500 years in the Hudson Valley (Cook et

al., 1999). We aim to provide a long-term water-level history for this highly-populated region by extending the longevity of the drought record, and by linking our results with those from the emerging array of other long-term high-resolution records.

Site Description and Methods

Davis Pond lies within the broad, slightly-sloping lowlands of the Housatonic River valley at the eastern margin of the Taconic Mountains, which forms the eastern edge of the Hudson River watershed in southwestern Massachusetts (Fig. 1). Surficial sediments are glacially-derived sand and gravel deposits (Norvitch, 1968), and overlie Cambrian–Ordovician-age Berkshire schist (Dale, 1923). A transitional hardwood conifer forest containing predominantly sugar maple (*Acer saccharum*) and red oak (*Quercus rubra*), with stands of hemlock (*Tsuga canadensis*) and white pine (*Pinus strobus*), surrounds the basin. Sweet peppercorn (*Clethra alterniflora*), holly (*Ilex opaca*), tamarack (*Larix laricina*) and herbaceous flora, including leatherleaf (*Chamaedaphne calyculata*), fringe the basin. Waterlilies (*Nuphar* and *Nymphaea* spp.) cover the pond in summer.

In the Northeast, the average January temperature (AD 2008) was -2.8°C , and 21.3°C in July (AD 1895-2008 January range -10.4 to 1.6°C ; July range 19.2 to 23.3°C). Regional average annual precipitation (AD 2008) was 1262 mm, about 58% higher than the annual average (729.9 mm) recorded during the final year of the AD 1962-65 drought in Massachusetts (www.nrcc.cornell.edu/page_summaries.html). Amidst the AD 1929-32 drought in southern New England, Kinnison (1931) noted lower-than-normal precipitation and depleted water supplies in numerous municipalities. Near Davis Pond, estimated departures from Hudson

Valley precipitation data between AD 1895 and 2005 show 28 (>6 month duration) droughts (Lyon et al., 2005).

Our approach to lake-level reconstruction (Newby et al., 2000; Newby et al., 2009; Shuman et al., 2001, 2005) is based on facies changes identified within a transect of sediment cores (Digerfeldt, 1986) and in ground-penetrating radar (GPR) profiles. Using a hand-driven piston corer, we obtained six sediment cores (Fig. 1) in AD 1999 at Davis Pond along a transect where GPR data were also collected using a GSSI SIR-2000 system with a 200-mhz antenna floated in a small raft (Fig. 2). The GPR profiles track changes in subsurface facies based on different dielectric constants within the sediments, but the signal at Davis Pond attenuates below about 5.0 m water depth and reveals only the upper portion of the stratigraphy.

We assume that fine-grained lacustrine silts captured in the cores and GPR profiles accumulated in deeper water than sand-rich sediments, which accumulate near the shore and extend into the basin during low water periods. Low sedimentation rates associated with sand-rich sediments provide further evidence of near-shore winnowing and erosion as expected if the deposition took place above wave base. Other factors could potentially transport sand into the pond, such as wind and surface run-off, but would be associated with high sedimentation rates. Additional transects of GPR data (not shown) indicate that the major sedimentary units identified in our cores also extend around the periphery of the basin, and thus confirm that these units are not the products of local slumps or surface water-flow. At present, the local topography has little to no gradient near the margin of the lake, and the lake is primarily fed by groundwater.

Laboratory analyses on the cores included loss-on-ignition (LOI) at contiguous 1-cm intervals to measure relative changes in sediment organic content (Dean, 1974). Based on the LOI of the core tops, we used 60% LOI (40% mineral content) as the boundary between the zones of lacustrine silt deposition offshore and sandy deposition in the near-shore littoral zone. To reconstruct the shoreline position through time, we track the position of sediments with >40% mineral content. Such sediments are commonly found in near-shore cores, such as B1.7, and rarely in off-shore cores, such as A100. Ten pollen samples from C-5 were processed using standard laboratory techniques (Faegri and Iversen, 1989), and a minimum of 200 grains were counted per sample at 400X. High-resolution (200 μm) x-radiographs of cores E40 and A100 were obtained using an ITRAX X-Ray Fluorescence (XRF) Core Scanner at Woods Hole Oceanographic Institution, and were examined to confirm that low LOI (<40%) intervals represented sand-rich sediments (Fig. 3). Visible sand layers in other cores were also documented with digital photography (Fig. 3).

Thirty-one samples of sediment or macrofossil material from the cores were submitted to the National Ocean Sciences Accelerator Mass Spectrometry (NOSAMS) facility to obtain radiocarbon dates (Table 1). We calibrated the dates for atmospheric radiocarbon variations using CALIB 5.0.2 (Reimer et al., 2004), and use the median calibrated ages throughout the text. The maximum and minimum of the 2σ calibrated age ranges represent the age span for each date in Table 1. We calculated sediment accumulation rates using the median ages.

Results

The radiocarbon-dated (Table 1) sediment cores span from ca.13.4 cal ka BP to present, and contain organic-rich (>60% LOI) sediments off-shore and sandy sediments near-shore (Figs. 3, 4). The boundaries between organic-rich and sandy deposition, however, fluctuated through time, thereby providing evidence for water-level changes. At least eleven sandy sediment units (I-XI; Fig. 4) in the different cores represent expansions of littoral sediment facies into the pond at times when lake levels declined (Fig. 5). Visible sand and gravel layers with low sedimentation rates define these units near shore, with synchronous declines in LOI and increases in the sand content representing the units in the most off-shore cores. Most of the units typically have several LOI minima, and likely represent multiple short-lived events.

Only a few intervals of organic sediment older than ca. 10.0 cal ka BP were recovered in the cores. In D20, however, a short sedimentary sequence of lacustrine silt interspersed with two distinct sand layers comprises the first two low water-level units (Fig. 3, 4). Unit I in D20 (Fig. 4) is located 627-623 cm below the modern lake surface (bmls), and is bracketed by two radiocarbon dates of 13.4 and 10.9 cal ka BP, which indicate a slow sediment accumulation rate of < 2 cm/kyr. A radiocarbon age above the Unit II sand layer (618-615 cm bmls) in D20 indicates that this low stand ended before ca. 10.4 cal ka BP, with sediment accumulating from the top of Unit I to the top of Unit II at 15.3 cm/kyr (Fig. 3). These accumulation rates, in Unit I and II, are lower than for any other portion of D20 (Table 1). Core A100 records Unit II as a steady decline in LOI after 10.6 cal ka BP, and E40 appears to contain Units I and II within sands below a radiocarbon age of 10.0 cal ka BP (Fig. 4).

The onset of lacustrine silt in E40 above the date of 10.0 cal ka BP (Fig. 5), and in D20 after 10.4 cal ka BP signals a brief rise in water levels (R1, Fig. 4) also recorded in A100 by a rise in LOI at 925 cm bmls. Both E40 and D20 then contain a series of low LOI intervals (Units III-VI) associated with sand deposition (Fig. 3), which we infer to represent low water levels that shifted sand to positions as deep as 819 cm bmls in E40 (Fig. 4). Two radiocarbon ages from E40 of 9.1 and 9.0 cal ka BP bracket two sandy layers (Fig. 3) within an interval of overall low LOI in Unit IV, and a radiocarbon age of 7.7 cal ka BP in D20 provides an age limit on the youngest portion of Unit V (Fig. 4). The sharp decline in LOI just above 7.7 cal ka BP in D20 represents the Unit VI lowstand (Fig. 4). After Unit VI, high LOI intervals in D20, E40 and A100 indicate a lack of sand transport into the basin at this time, while the onset of lacustrine silt deposition at the base of F10 around 6.6 cal ka BP shows that water levels rose during this 1100 yr interval (R2, Fig. 4).

After 6.6 cal ka BP, water levels dropped and sand accumulated as far into the basin as A100 (Unit VII, Fig. 3), as indicated by declines in LOI to 40-60% (Unit VII) in F10, D20, E40 and A100 above radiocarbon ages of 6.6-6.4 cal ka BP (Fig. 4). After the deposition of Unit VII, water levels rose (R3, Fig. 4) but then fell by ca. 5.6 cal ka BP, as indicated by sand layers and low LOI (Unit VIII) in C5, F10, D20, E40 and A100 (Fig. 4). The GPR data also show a bright reflector that truncates older sediments, and is consistent with the Unit VIII sand layer at the locations of C5 and F10 (Fig. 2). Radiocarbon ages of 5.6 and 4.9 cal ka BP in F10 best constrain the age of Unit VIII, and bracket the larger and upper of two sand layers within the unit (Fig. 4). These ages also confirm a slow sediment accumulation rate across Unit VIII (30.0

cm/kyr) compared to most of F10 (Table 1). A radiocarbon age of 4.7 cal ka BP at the upper boundary of Unit VIII in D20 is consistent with the F10 dates (Fig. 4).

The data from F10 and the GPR profile indicate that the Unit VIII sands, deposited from 5.6-4.9 cal ka BP, may represent the driest interval in the past 6.6 cal ka BP (Fig. 5). A sand layer in C5 at 190-180 cm bmls, below the radiocarbon age of 5.7 cal ka BP, may also record the Unit VIII low stand (Fig. 4). We surmise that this radiocarbon age should be ca. 4.9 cal ka BP, based on stratigraphic correlations with sand layers in F10 (4.9 cal ka BP) and D20 (4.7 cal ka BP). The 5.7 cal ka BP age from the radiocarbon-dated sample from C5 probably contained older reworked material. Two pollen samples (Fig. 6) from above the 5.6 cal ka BP radiocarbon date in C5 both contain high (38%) oak (*Quercus*) and low (1.5%) hemlock (*Tsuga*) pollen, and support our inference because regional pollen data only contain such low hemlock pollen percentages after 5.4 cal ka BP (Oswald et al., 2007).

After ca. 4.9 cal ka BP, the onset of lacustrine silt deposition above the Unit VIII sand layers in C5 and in F10 marks the next rise in water levels (R4, Fig. 4) at Davis Pond (Fig. 5).

Radiocarbon dates of 4.9 and 3.4 cal ka BP indicate an increase in sediment accumulation rates to >60 cm/kyr in F10 at this time (Fig. 4), which further supports the inferred rise. During this rise, a series of drops in LOI (Unit IX) after 4.9 cal ka BP in F10 (at 247 and 235 cm bmls), D20 (at 352 cm bmls), E40 (at 414 cm bmls) and A100 (at 476 cm bmls; Fig. 3) indicate brief low stands, but these intervals are not well constrained by radiocarbon dates (Fig. 4).

By ca. 3.5 cal ka BP, water levels fell substantially based on sand and gravel layers (Unit X; Fig. 3-5), which are bounded by radiocarbon ages of 3.5 cal ka BP in C5 (145 cm bmls) and 3.4 cal ka BP in F10 (190 cm bmls)(Fig. 4). In C5, Unit X contains two coarse gravel layers below a date of 2.3 cal ka BP, and a radiocarbon age of 3.0 cal ka BP obtained from the high-LOI silts between the layers may indicate a brief high stand (Fig. 5). Sediment accumulation rates in F10 drop to their lowest value (22.7 cm/kyr) in association with Unit X, e.g. compare with 30.0 cm/kyr in Unit VIII from 5.6-4.9 cal ka BP and ca. 40-70 cm/kyr for most other portions of the core (Table 1). Unit X also appears in the GPR data as a bright reflector at the approximate depth of the sand and gravel layers in C5 and F10 (Fig. 2). Based on these results, Unit X appears to represent the most substantial or frequent drought of the past 4.9 cal ka BP (Fig. 5).

After 2.3 cal ka BP, rising water levels are recorded by intervals with high LOI in all the cores, including B1.7 (R5, Figs. 4, 5). The timing of this rise in LOI is best constrained by a radiocarbon date in C5 of 2.3 cal ka BP (118 cm bmls). A terrace surrounding the pond at ~0.5 m above the modern lake surface attests to at least one former period when the pond reached higher than modern levels, but the C5 and B1.7 cores indicate that near-modern levels have only persistently existed since ca. 2.3 cal ka BP. The low-stand deposits associated with Unit XI interrupt this “high-stand” evidence (Fig. 5), and are defined by low-LOI sediments from 94-51 and 148-76 cm bmls in C5 and F10 respectively (Fig. 4). GPR data show a significant reflector near the position of B1.7, which may represent Unit XI (Fig. 2). Radiocarbon ages from F10 and A100 indicate that this low stand (Unit XI) began at ca. 1.6 cal ka BP, and a radiocarbon age in F10 constrains the end of the event to be after 0.6 cal ka BP.

Discussion

Two features of the Davis Pond record provide insight into the regional hydroclimate over the past 13,000 years: evidence of a long-term rise and repeated short-term low-stands. The low stands are superimposed on the overall trend toward higher water levels after ca. 10.4 cal ka BP (Unit II), which is evident from the progressively younger basal ages of F10 and C5 (Figs. 4, 5). From ca. 10.4 to 6.6 cal ka BP (Units II-VI), the paleoshoreline fluctuated between 20 and 40 m from the modern shore with sediments only accumulating in cores D20, E40 and A100. After 6.6 cal ka BP (Unit VII), F10 began to accumulate sediment as Davis Pond expanded to within 10 m of the modern shoreline. By ca. 4.9 cal ka BP, silts began to accumulate in C5 and the shoreline fluctuated among locations within 5-10 m of the modern shore (during the deposition of Units VII-XI). We infer the modern shoreline was likely reached by ca. 2.3 cal ka BP when silt began to accumulate in B1.7 (Fig. 4).

The long-term tendency toward high water levels in the Davis Pond (Fig. 5) may be explained by seasonal insolation trends during the Holocene, which drove atmospheric circulation changes that likely contributed to an increase in effective moisture in the region throughout the Holocene (Diffenbaugh et al., 2006). The direct effects of the insolation trends would have also caused a progressive decline in evaporation rates since before 10.4 cal ka BP (Webb et al., 1998). Furthermore, an increase in water levels after ca. 8.0 cal ka BP (Unit V) conforms with the inference (Shuman et al., 2002) that lake levels rose in New England after the collapse of the Hudson Bay ice dome ca. 8.2 cal ka BP. Regional conditions then moistened as subtropical moisture was readily advected northward.

In addition to the long-term trend, the eleven low stand units (many containing multiple individual event layers) indicate the regional importance of multi-century hydroclimatic variability consistent with that inferred from an emerging group of recent studies (Li et al., 2007; Newby et al., 2009). In southeastern Massachusetts, multiple sand layers in the sediment stratigraphies of Rocky and New Long Ponds record repeated Pleistocene and Holocene low stands (Newby et al., 2009; Shuman et al., 2009). The ages of these low stands overlap with those identified here: Unit I (13.4-10.9 ka) at Davis Pond overlaps in time with early low stands at Rocky and New Long Ponds during the Younger Dryas; Unit II (10.9-10.4 ka) at Davis Pond correlates in time with low-stand sand layers at Rocky and New Long Ponds dating to 11.0-10.2 cal ka BP and before 10.3 cal ka BP respectively; Units IV and V at Davis Pond coincide in time with sand layers at Rocky and New Long Ponds that indicate low-water levels during the 9.2 cal ka BP (Fleitmann et al., 2008) and the 8.2 cal ka BP (Alley et al., 1997) events. After ca. 6.0 cal ka BP, the record at Rocky Pond is poorly resolved but the ages of Davis Pond low-stand continue to overlap with those at New Long Pond from 5.7-1.2 cal ka BP: Davis Pond Unit VIII (5.6-4.9 cal ka BP) coincides with a New Long Pond low stand at 5.7-4.9 cal ka BP, Davis Pond Unit IX (before 3.5 cal ka BP) corresponds to a New Long Pond low stand at 4.1-3.6 cal ka BP, Davis Pond Unit X (3.0-2.3 cal ka BP; likely two events before and after 2.7 cal ka BP) overlaps to two New Long Pond low stands at 3.6-2.7 and 2.5-1.9 cal ka BP, and Davis Pond Unit XI (1.6-0.6 cal ka BP) correlates with one at New Long Pond at 1.9-1.2 cal ka BP. Further afield, the four low-stand intervals at White Lake in New Jersey (Li et al., 2007) also correspond in time with Units VIII-XI at Davis Pond. Taken together, the regional network of datasets appears to coherently indicate numerous century-scale and longer droughts in New England during the Holocene.

In addition, the similar timing of low stands during the late-Pleistocene and early-Holocene at multiple lakes in New England indicates a possible link between drought and abrupt temperature changes in the North Atlantic region, such as during the Younger Dryas, 9.2 cal ka BP, and 8.2 cal ka BP events (Newby et al., 2009). As noted by Li et al. (Li et al., 2007), the influence of the North Atlantic Ocean may have continued to play an important role in forcing prolonged regional droughts during the remainder of the Holocene, just as it did in the most severe historic drought in AD 1962-1966 (Namias, 1966). For example, the coincident low stands at Davis Pond (esp. Units V, VIII, and IX) and New Long Pond are also synchronous with cold episodes in Greenland (Shuman et al., 2009). The Davis Pond data, thus, appear consistent with Newby et al.'s (Newby et al., 2009) suggestion that changes in Atlantic Meridional Overturning Circulation and sea-surface temperatures off the coast of New England may be an important mechanism for initiating long-term drought periods in the region.

Conclusion

Our detailed multi-core record from Davis Pond includes well resolved evidence of hydrological changes that show high-frequency changes superimposed on previously-documented, multi-millennial changes in moisture conditions during the late-Quaternary in New England. The recent AD 1960s drought showed how such events impact natural systems (streamflow, lake levels and groundwater) and human needs (agriculture, water supply). Our data confirm the potential for regional changes with similar consequences in the future, if regional drought frequency increases as climate models project for the end of this century, driven by increased evaporation across the northeastern United States (Hayhoe et al., 2007). Enhanced evaporation

compared to today during the early-Holocene may similarly explain the particularly low water levels at Davis Pond before 6.6 cal ka BP, and thus sets a precedent for the predicted future changes. Our results also confirm that the regional hydroclimate may be more variable than experienced historically, and that multiple droughts of different magnitude and longevity have accompanied past climatic changes and could do so in the future. In particular, the apparent sensitivity of regional water supplies to conditions in the North Atlantic raises concerns about the hydrologic impacts of potential future changes in oceanic circulation (Alley et al., 2003). Thus, our data underscore the potential for future climate change to impact the water resources of this highly populated region.

Acknowledgements

We thank The Ocean and Climate Change Institute at Woods Hole Oceanographic Institution and NSF Earth System History program grants (EAR-0602380 to J. Donnelly and EAR-0602408 to B. Shuman) for supporting this research. P. Leduc, J. Tierney, M. Gomes, J. Williams and B. Zipser skillfully assisted in the field and laboratory. We thank L. Carlson for Geographic Information Systems work and G. Smith for his enthusiasm and for granting access to the pond.

References

- Alley, R. B., Marotzke, J., Nordhaus, W. D., Overpeck, J. T., Peteet, D. M., Pielke, R. A., Jr., Pierrehumbert, R. T., Rhines, P. B., Stocker, T. F., Talley, L. D., and Wallace, J. M. (2003). Abrupt Climate Change. *Science* **299**, 2005-2010.
- Alley, R. B., Mayewski, P. A., Sowers, T., Stuiver, M., Taylor, K. C., and Clark, P. U. (1997). Holocene climatic instability: A prominent, widespread event 8200 yr ago. *Geology* **25**, 483-486.
- Almquist, H., Dieffenbacher-Krall, A. C., Flanagan-Brown, R., and Sanger, D. (2001). The Holocene record of lake levels of Mansell Pond, central Maine, USA. *The Holocene* **11**, 189-201.
- Andrews, J. F. (1965). The weather and circulation of July 1965. *Monthly Weather Review* **93** (10), 647-654.
- Cook, E. R., Meko, D. M., Stahle, D. W., and Cleaveland, M. K. (1999). Drought reconstructions for the continental United States. *Journal of Climate* **12**, 1145-1162.

- Dale, T. N. (1923). The Lime Belt of Massachusetts and Parts of Eastern New York and Western Connecticut. United States Geological Survey, Bulletin **744**, Washington DC, 71 pp.
- Dean, W. E. (1974). Determination of carbonate and organic matter in calcareous sediments and sedimentary rocks by loss on ignition: comparison with other methods. *Journal of Sedimentary Petrology* **44**, 242-248.
- Degaetano, A. T. (1999). A Temporal Comparison of Drought Impacts and Responses in the New York City Metropolitan Area. *Climatic Change* **42**, 539-560.
- Dieffenbacher-Krall, A. C., and Nurse, A. M. (2005). Late-Glacial and Holocene Record of Lake Levels of Mathews Pond and Whitehead Lake, Northern Maine, USA. *Journal of Paleolimnology* **34**, 283-309.
- Diffenbaugh, N. S., Ashfaq, M., Shuman, B., Williams, J. W., and Bartlein, P. J. (2006). Summer aridity in the United States: Response to mid-Holocene changes in insolation and sea surface temperature. *Geophysical Research Letters* **33**, L22712.
- Digerfeldt, G. 1986. Studies on past lake-level fluctuations, *in* Berglund, B.E., ed., Handbook of Holocene palaeoecology and palaeohydrology: John Wiley and Sons, Chichester, United Kingdom, p. 127–142.
- Faegri, K. and Iversen J. (1989). Textbook of Pollen Analysis. (4th edn). John Wiley and Sons, Chichester, 328 pp.
- Fleitmann, D., Mudelsee, M., Burns, S. J., Bradley, R. S., Kramers, J., and Matter, A. (2008). Evidence for a widespread climatic anomaly at around 9.2 ka before present. *Paleoceanography* **23**, PA1102.
- Griffith, G. E., Omernik, J. M. Pierson, S. M. and Kiilsgaard, C. W. (1994). The Massachusetts

ecological regions project. United States Environmental Protection Agency, Publication No. 17587-74-6/94-DEP, Washington D. C.

Hayhoe, K., Wake, C., Huntington, T., Luo, L., Schwartz, M., Sheffield, J., Wood, E., Anderson, B., Bradbury, J., DeGaetano, A., Troy, T., and Wolfe, D. (2007). Past and future changes in climate and hydrological indicators in the US Northeast. *Climate Dynamics* **28**, 381-407.

Hill, T. D., and Polsky, C. (2007). Suburbanization and drought: A mixed methods vulnerability assessment in rainy Massachusetts. *Environmental Hazards* **7**, 291-301.

Kinnison, H. B. (1931). The 1929-1930 Drought in New England. . *Journal of New England Water Works Association* **45**, 145-163.

Kirby, M., Patterson, W., Mullins, H., Burnett, and Burnett, A. (2002). Post-Younger Dryas climate interval linked to circumpolar vortex variability: isotopic evidence from Fayetteville Green Lake, New York. *Climate Dynamics* **19**, 321-330.

Leathers, D. J., Grundstein, A. J., and Ellis, A. W. (2000). Growing season moisture deficits across the northeastern United States. *Climate Dynamics* **14**, 43-55.

Li, Y.-X., Yu, Z., and Kodama, K. P. (2007). Sensitive moisture response to Holocene millennial-scale climate variations in the Mid-Atlantic region, USA. *The Holocene* **17**, 3-8.

Lyon, B., Christie-Blick, N. and Gluzberg, Y. (2005). Water shortages, development, and drought in Rockland County, New York. *Journal of the American Water Resources Association (JA)* **41** (6), 1457-1469.

Maenza-Gmelch, T. E. (1997). Holocene vegetation, climate, and fire history of the Hudson Highlands, southeastern New York, USA. *The Holocene* **7**, 25-37.

- Namias, J. (1966). Nature and possible causes of the northeastern United States drought during 1962-65 *Monthly Weather Review* **94**, 543-554.
- Newby, P. C., Killoran, P., Waldorf, M., Shuman, B. N., Webb, T., III, and Webb, R. S. (2000). 14,000 years of sediment, vegetation, and water level changes at the Makepeace Cedar Swamp, southeastern Massachusetts. *Quaternary Research* **53**, 352-368.
- Newby, P. E., Donnelly, J. P., Shuman, B. N., and MacDonald, D. (2009). Evidence of centennial-scale drought from southeastern Massachusetts during the Pleistocene/Holocene transition. *Quaternary Science Reviews* **28**, 1675-1692.
- Norvitch, R. F., and Lamb, M. E. S. (1966). Housatonic River Basin, United States Geological Survey Massachusetts Basic-Data Report **9**, Ground-Water Series, Washington D. C., 40 pp.
- Oswald, W. W., Faison, E. K., Foster, D. R., Doughty, E. D., Hall, B. R., and Hansen, B. C. S. (2007). Post-glacial changes in spatial patterns of vegetation across southern New England. *Journal of Biogeography* **34**, 900-913.
- Peteet, D. M., Vogel, J. S., Nelson, D. E., Southon, J. R., Nickmann, R. J., and Heusser, L. E. (1990). Younger Dryas climatic reversal in northeastern USA? AMS ages for an older problem. *Quaternary Research* **33**, 219.
- Reimer, P. J., Baillie, M. G. L., Bard, E., Bayliss, A., Beck, J. W., Bertrand, C. J. H., Blackwell, P. G., Buck, C. E., Burr, G. S., Cutler, K. B., Damon, P. E., Edwards, R. L., Fairbanks, R. G., Friedrich, M., Guilderson, T. P., Hogg, A. G., Hughen, K. A., Kromer, B., McCormac, F. G., Manning, S. W., Ramsey, C. B., Reimer, R. W., Remmele, S., Southon, J. R., Stuiver, M., Talamo, S., Taylor, F. W., van der Plicht, J., and

- Weyhenmeyer, C. E. (2004). IntCal04 Terrestrial radiocarbon age calibration, 26 - 0 ka BP. *Radiocarbon* **46**, 1029.
- Shuman, B., Bravo, J., Kaye, J., Lynch, J. A., Newby, P., and Webb, T., III. (2001). Late-Quaternary water-level variations and vegetation history at Crooked Pond, southeastern Massachusetts. *Quaternary Research* **56**, 401-410.
- Shuman, B., Newby, P., Donnelly, J. P., Tarbox, A., and Webb, T., III. (2005). A Record of Late-Quaternary Moisture-Balance Change and Vegetation Response from the White Mountains, New Hampshire. *Annals of the Association of American Geographers* **95**, 237-248.
- Shuman, B. N., Bartlein, P. J., Logar, N., Newby, P., and Webb, T., III. (2002). Parallel climate and vegetation responses to the early Holocene collapse of the Laurentide Ice Sheet. *Quaternary Science Reviews* **21**, 1793-1805.
- Shuman, B. N., Newby, P., and Donnelly, J. P. (2009). Abrupt climate change as an important agent of ecological change in the Northeast U.S. throughout the past 15,000 years. *Quaternary Science Reviews* **28**, 1693-1709.
- Webb, R. S., Anderson, K. H., and Webb, T. (1993). Pollen Response-Surface Estimates of Late-Quaternary Changes in the Moisture Balance of the Northeastern United States. *Quaternary Research* **40**, 213-227.
- Webb, T., III, Anderson, K. H., Webb, R. S., and Bartlein, P. J. (1998). Late Quaternary climate changes in eastern North America: a comparison of pollen-derived estimates with climate model results. *Quaternary Science Reviews* **17**, 333-357.

Figure Legends

Figure 1. Location of Davis Pond (circle) in southwestern Massachusetts within Housatonic River watershed (dark line). Nearby are the Hudson River watershed (dotted line) and New York City's water reservoirs (boxed labels 1-Catskills/Delaware Watersheds and 2-Groton Watershed). Lower left: location of GPR transect with six cores in this study. Lower right: location of sites in text: 1-Davis Pond, 2-Fayetteville Green Lake (Kirby et al., 2002), 3-Rocky and New Long Ponds (Newby et al., 2009; Shuman et al., 2009) and 4-White Pond (Li et al., 2007).

Figure 2. Davis Pond GPR schematic and profile. Vertical white lines show locations of D20, F10, C5 and B1.7. Dark horizontally-oriented lines outline GPR reflectors; low stand Units VII-XI are described in the text.

Figure 3. Digital and radiographic images from Davis Pond. Digital images from D20 (Units I and II) and C5 (Unit X) show sand and gravel (respectively) deposits. Light (dense) portions of x-radiographic (200 μ m resolution) images from A100 and E40 reveal sand fractions within lacustrine sediments. Further details on radiocarbon ages (\blacktriangleright ; cal ka BP) are in Table 1. In Fig. 4, Unit III (E40) is displayed as two sand layers and Unit V as one sand layer.

Figure 4. Correlation among low stand Units I-XI and LOI by depth in Davis Pond, with radiocarbon dates (\blacktriangleleft , cal ka BP; cm bmls). Left of vertical dashed lines show sandy (<40% organic) mineral-rich sediments, which as expected, become increasingly inorganic closer to the shore. The upper meter (dashed box) of D20 was not collected.

Figure 5. Changes in water level at Davis Pond by age (cal ka BP). A. Gray bands show low-stand Units I-XI on percent mineral fraction in A100; note that the youngest event in Unit VIII overlaps a core break. B. Changes in water level displayed by extensions of sand (gray) from modern shore into the basin for each Unit. R1-R5 indicate rises in water level as per text.

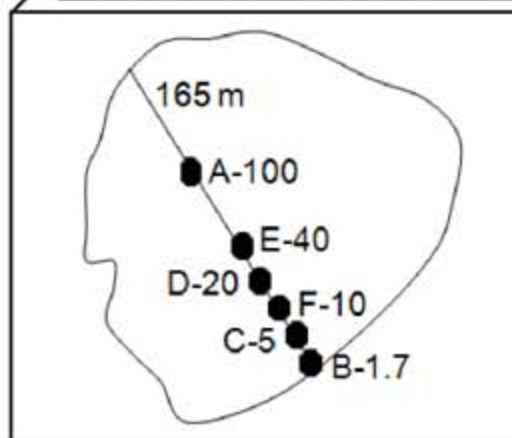
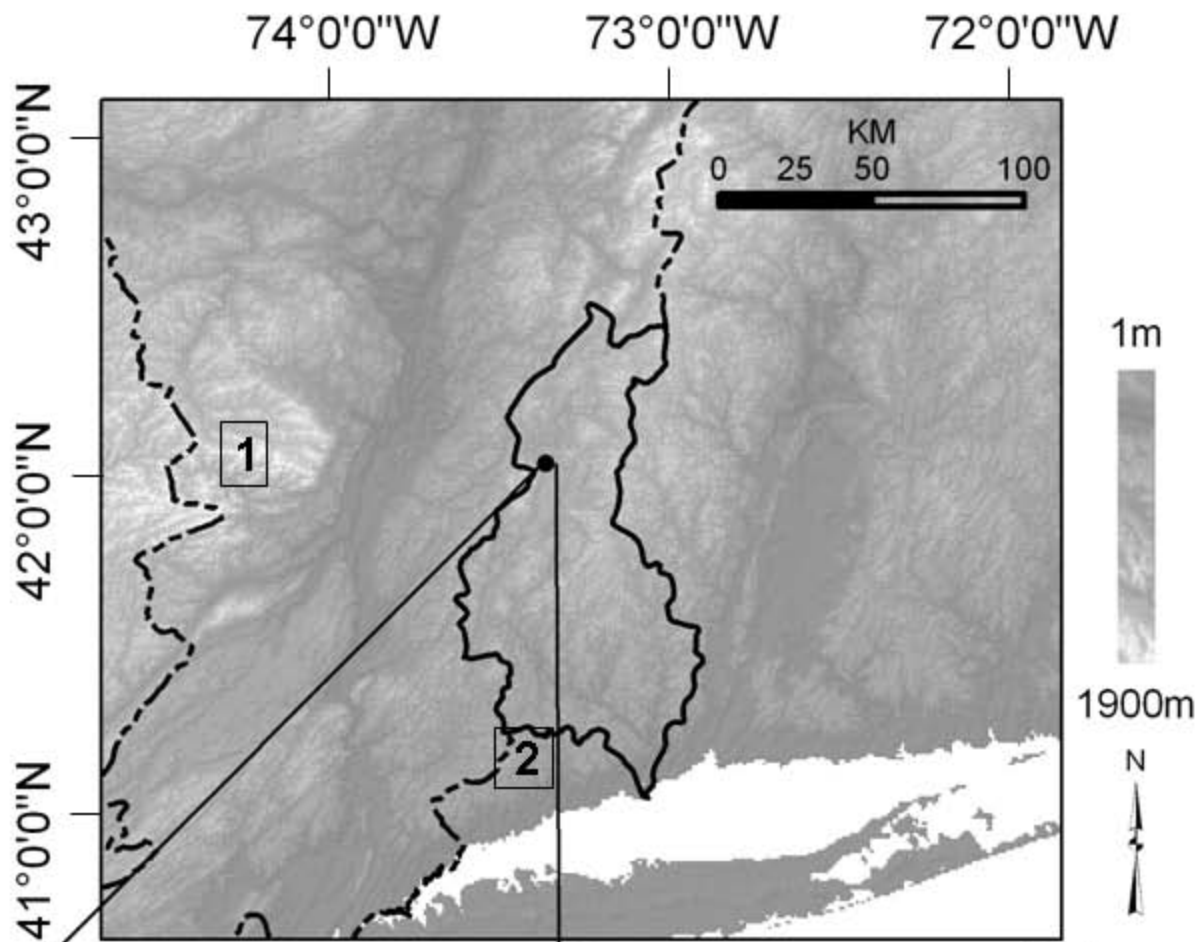
Figure 6.

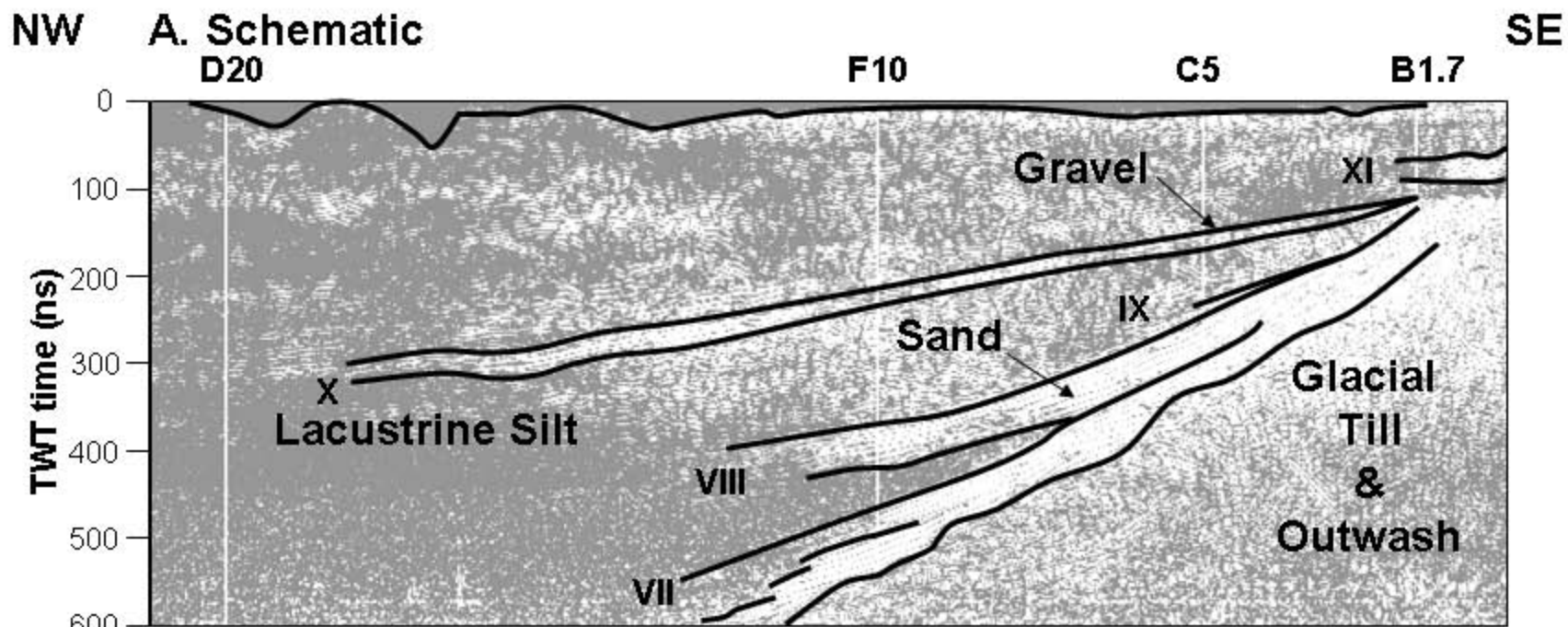
Table Legends

Table 1 Radiocarbon Dates and Sedimentation Rates

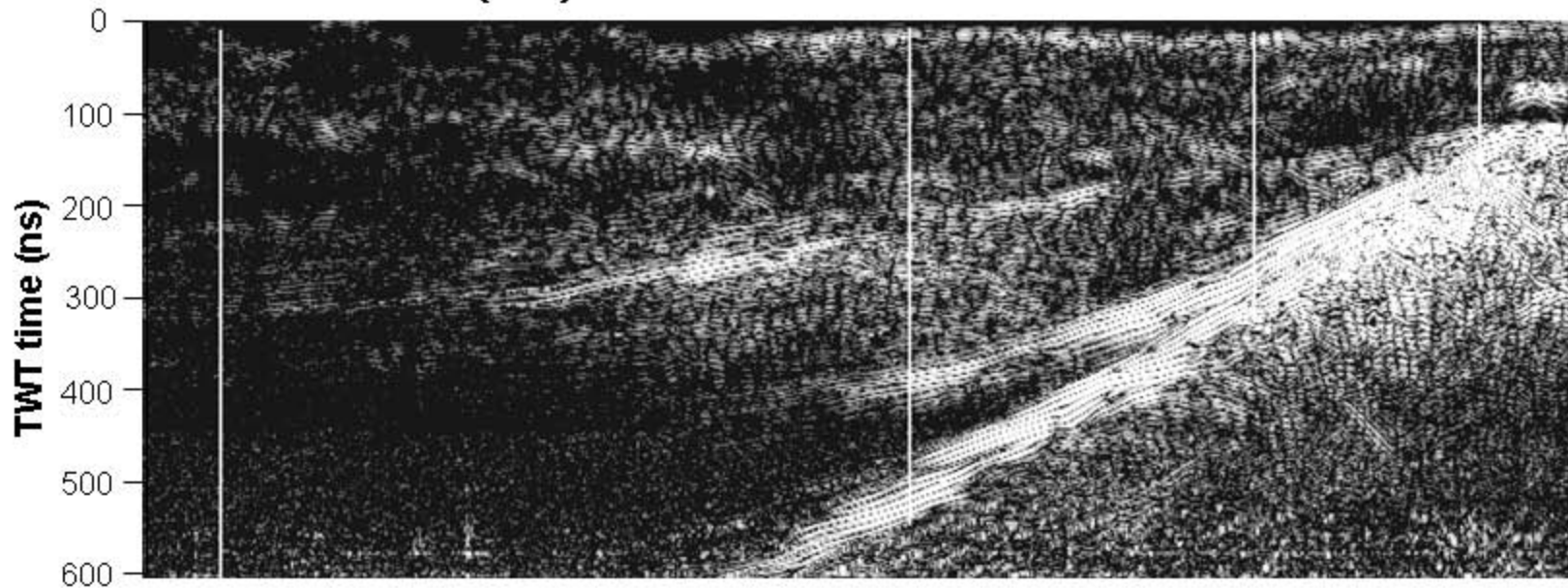
*bmls: below modern lake surface.

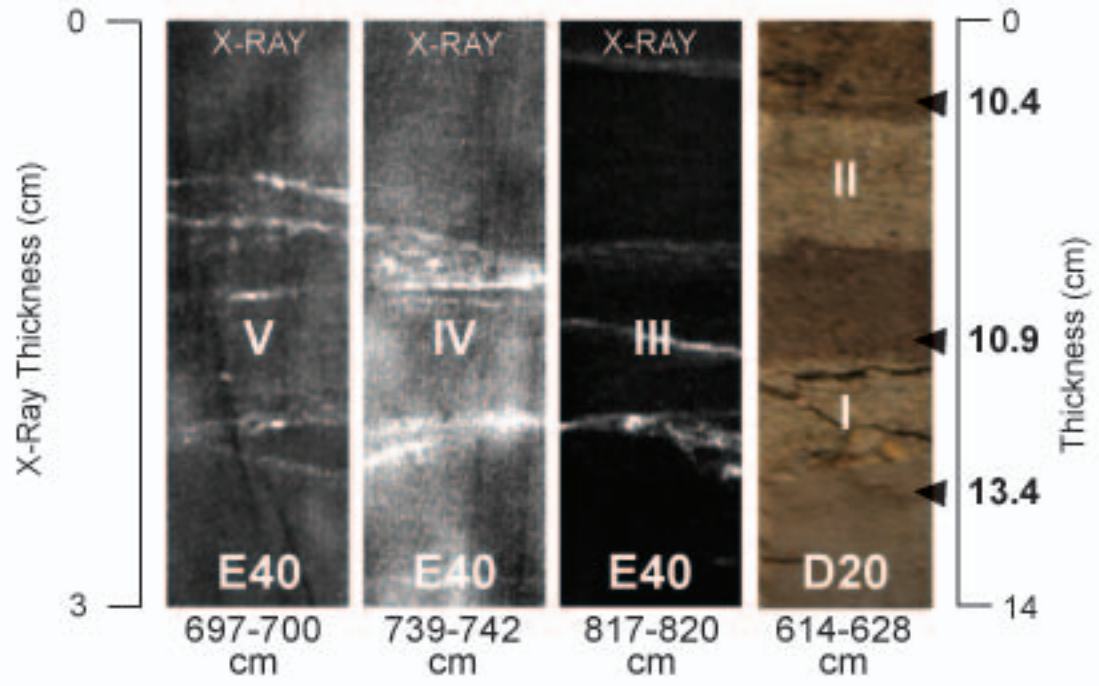
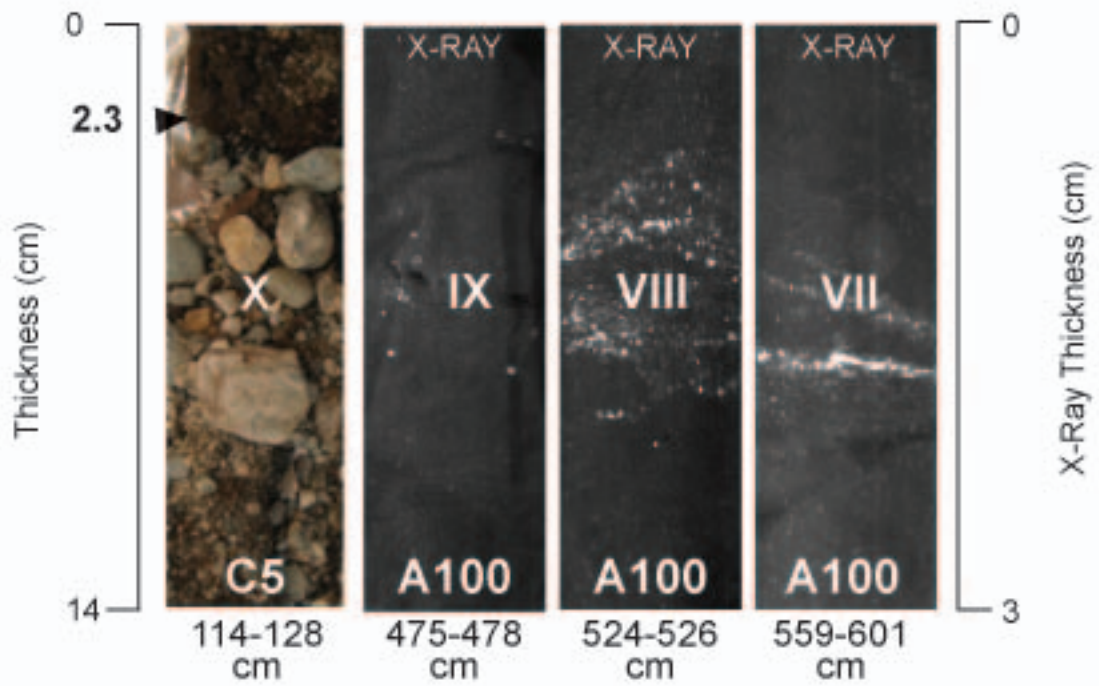
**Material Dated: 1-Bulk Sediment, 2-Bulk Sediment with Fibrous Material, 3-Macrofossils, 4-Seed, 5-Fine Rootlets, 6- Rootlets and Algae, 7-Sedge (*Carex* sp. Fragments), 8-Sediment with Organics, 9-Plant/Wood, 10-Wood, 11-Cone Scales.

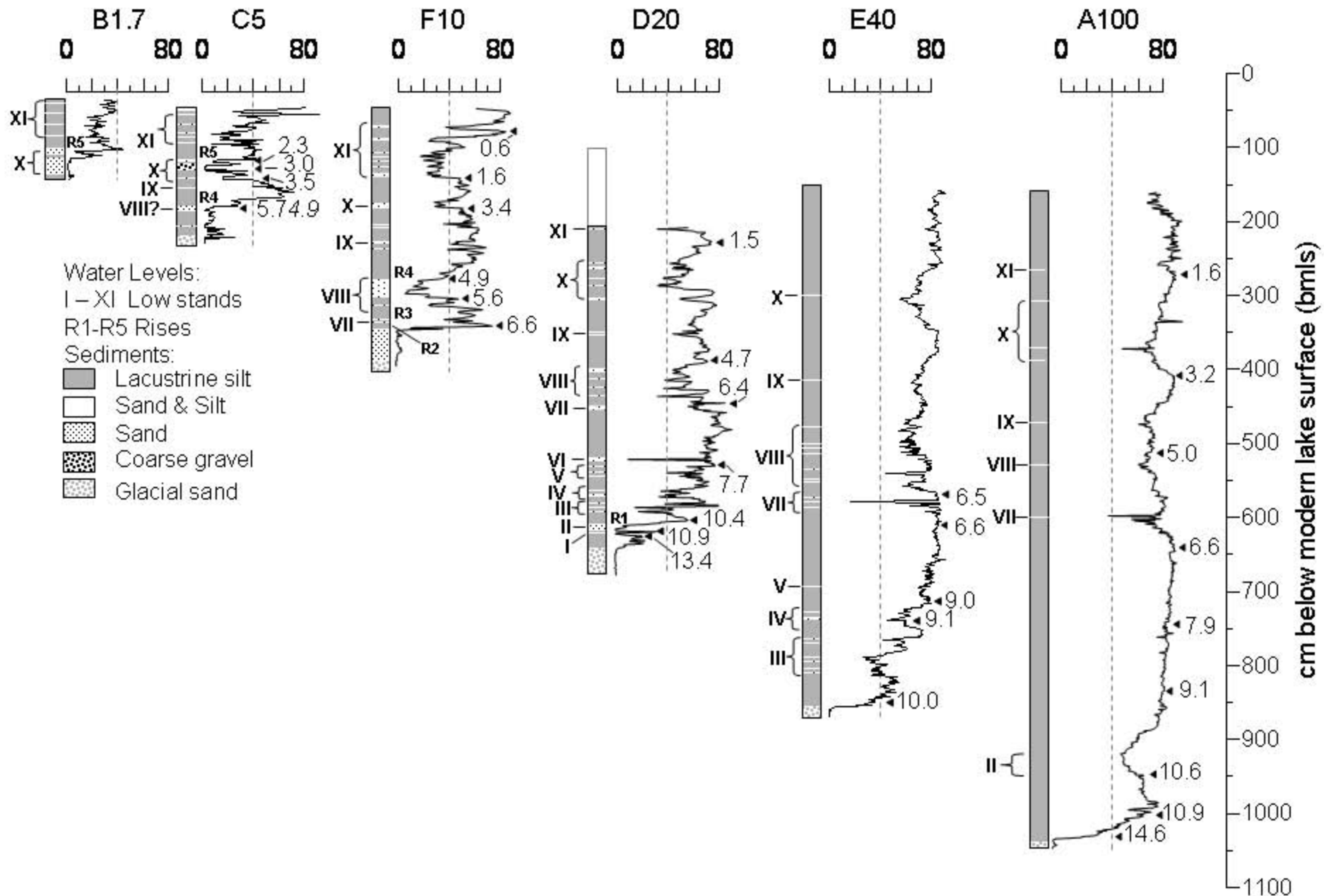




B. GPR Profile (T-4)



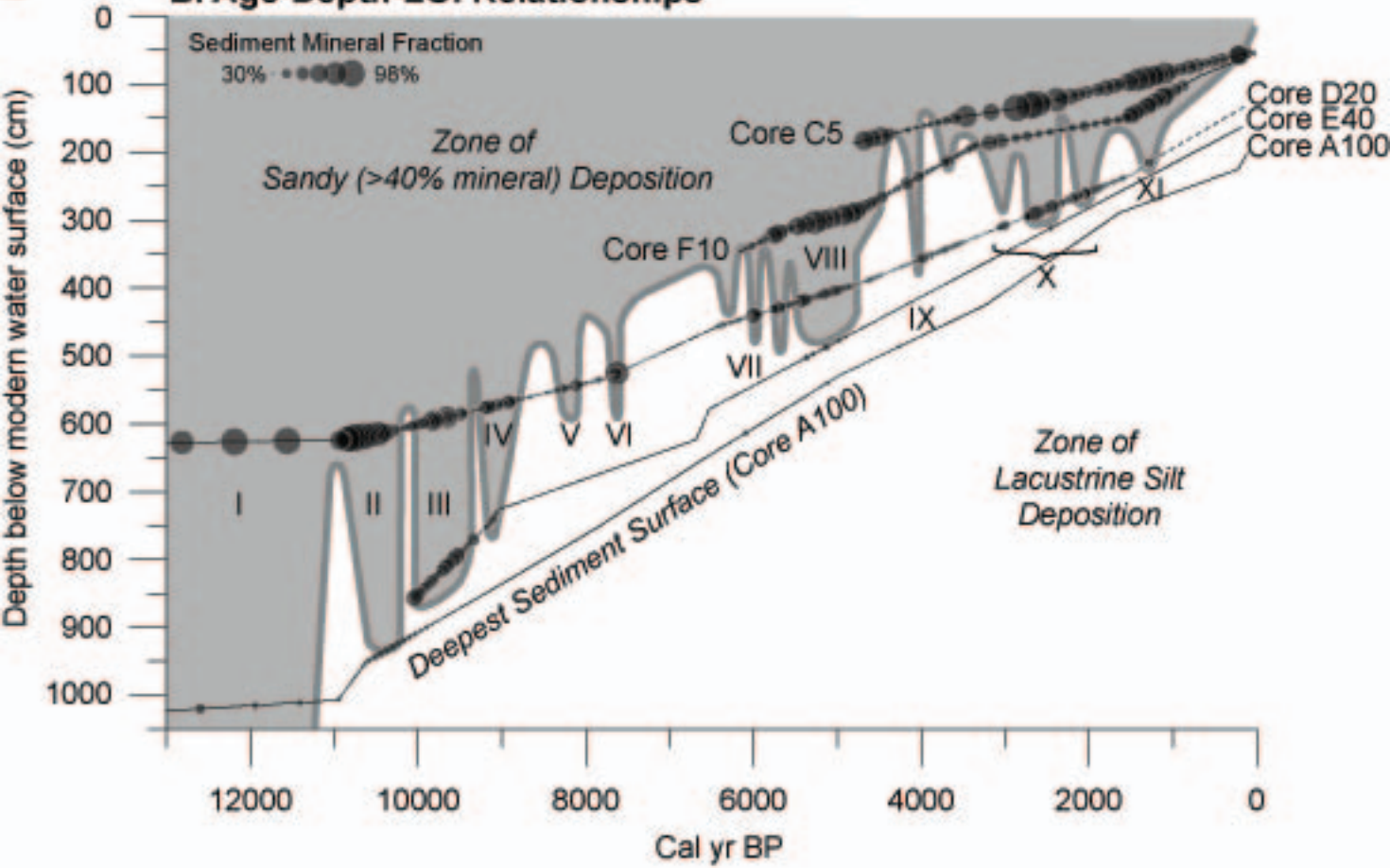




A. Core A100 LOI



B. Age-Depth-LOI Relationships



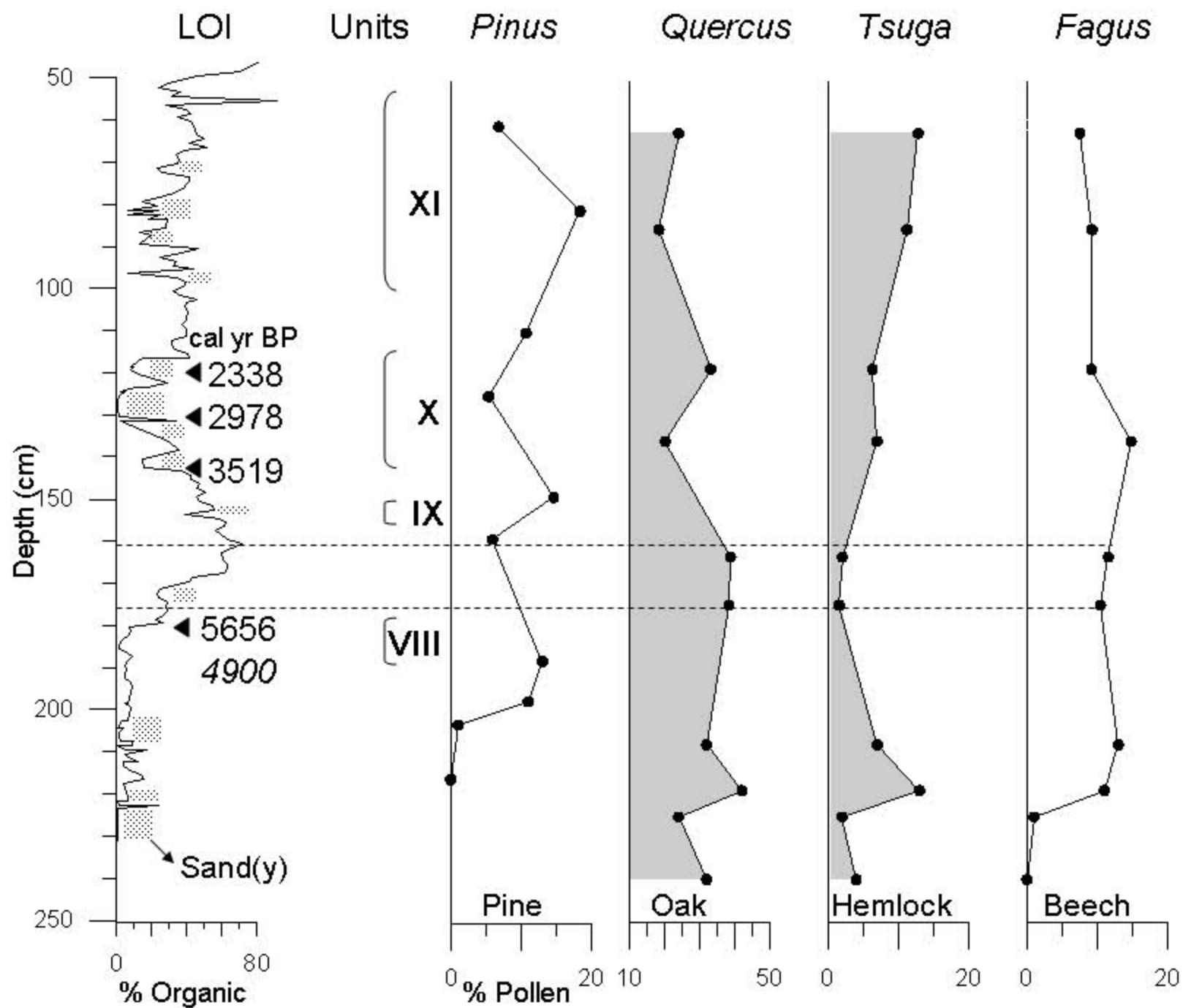


Table 1. Radiocarbon Dates and Sedimentation Rates

No.	Core	Depth (cm) bmls*	NOSAMS Lab No.	¹⁴ C yr BP	Age error	Calib Median cal yr BP	Calib Low cal yr BP	Calib High cal yr BP	Material Dated**	Sedimentation Rates cm/kyr
1	A	276.5	OS-58072	1720	30	1629	1554	1704	1	69.7
2	A	414.5	OS-58073	3020	35	3234	3080	3341	2	86.0
3	A	519.5	OS-57913	4400	30	4962	4866	5211	3	60.8
4	A	647.5	OS-58068	5820	45	6626	6502	6731	1	76.9
5	A	748.5	OS-59706	7030	40	7872	7763	7953	2	81.1
6	A	838.5	OS-58065	8150	40	9086	9007	9252	1	74.1
7	A	949.5	OS-58066	9390	55	10621	10439	10754	1	72.3
8	A	1006.5	OS-59530	9630	45	10953	10778	11179	4	171.7
9	A	1034.5	OS-55125	12500	50	14624	14245	14952	1	7.6
10	C	118.5	OS-38532	2310	30	2338	2183	2358	5	28.7
11	C	129.5	OS-38533	2860	30	2978	2878	3073	5	17.2
12	C	144.5	OS-58074	3290	40	3519	3412	3630	1	27.7
13	C	180.5	OS-58027	4930	45	5656	5589	5745	1	16.8
14	D	232.5	OS-54852	1590	40	1471	1389	1557	6	89.4

15	D	391	OS-54983	4140	35	4684	4537	4824	1	49.3
16	D	455	OS-54984	5620	40	6397	6310	6479	1	37.4
17	D	532.5	OS-60578	6920	40	7748	7674	7839	1	57.4
18	D	615	OS-38531	9240	40	10409	10262	10543	1	31.0
19	D	623	OS-55126	9570	40	10933	10736	11100	7	15.3
20	D	627	OS-38790	11600	60	13440	13302	13618	1	1.6
21	E	578.5	OS-60128	5730	40	6527	6414	6637	1	65.3
22	E	623.5	OS-59968	5860	40	6683	6562	6779	8	288.5
23	E	726.5	OS-58071	8100	50	9041	8780	9253	1	43.7
24	E	744.5	OS-55124	8180	45	9125	9016	9268	1	214.3
25	E	856.5	OS-60577	8940	60	10050	9828	10233	1	121.1
26	F	86.5	OS-57908	735	30	679	657	726	9	46.0
27	F	149.5	OS-57909	1700	25	1603	1540	1693	9	68.2
28	F	189.5	OS-57910	3130	25	3363	3267	3439	9	22.7
29	F	289.5	OS-54867	4300	50	4871	4829	4959	5	66.3
30	F	312.5	OS-54985	4920	30	5638	5595	5715	10	30.1
31	F	348.5	OS-55039	5700	290	6524	5908	7243	11	40.6

